

Experimental evidence for nematic order of cuprates in relation to lattice structure

David J. Singh

Materials Science and Technology Division, Oak Ridge National Laboratory, Oak Ridge, Tennessee 37831-6114

I. I. Mazin

Code 6690, Naval Research Laboratory, Washington, DC 20375

(Dated: July 8, 2010)

Experiments that have been interpreted as providing evidence that the pseudogap phase in cuprates is an electronic nematic are discussed from the point of view of lattice structure. We conclude that existing experiments are not sufficient to prove a nematic origin of the pseudogap in underdoped cuprates.

PACS numbers: 74.72.Kf

I. INTRODUCTION

Understanding the nature of the pseudogap¹⁻⁵ and its relationship to superconductivity has emerged as a central problem in high T_c cuprate superconductivity. While there has been considerable progress in elucidating its momentum and doping dependence, its microscopic origin and relationship to superconductivity remain controversial. Some widely discussed experimentally supported possibilities are (1) that it is associated with an order with a quantum critical point below the superconducting dome that may play a key role in superconductivity and normal state transport.^{6,7} (2) that it represents Cooper pairing without phase coherence, i.e. a strong coupling precursor of superconductivity,⁸ and in contrast (3) that it is a phase associated with cuprates that competes with superconductivity.^{9,10} There have also been recent discussions, also based on experimental results, of the pseudogap phase as an electronic nematic, specifically associating the pseudogap temperature T^* with an onset of electronic nematicity.¹¹⁻¹⁵ The purpose of this paper is to discuss the experimental evidence for this. We argue that, contrary to recent suggestions,¹¹ the evidence for an association of T^* with an onset of nematic order is actually weak.

We emphasize that we are not discussing the so-called stripes in the strongly underdoped 214 cuprates. Theoretically, these are a dynamic phase separation that minimizes the Coulomb energy, and they occur on a larger length scale than the microscopic nematicity that is thought to occur in $\text{Sr}_3\text{Ru}_2\text{O}_7$ and above T_{AFM} in pnictides.

Specifically, we analyze the statement that at the temperature T^* where a pseudogap in the excitation spectrum develops the symmetry the CuO_2 plane(s) breaks from a four-fold (tetragonal) to at most a two-fold. The experiments that seem to support this idea include transport measurements on $\text{YBa}_2\text{Cu}_3\text{O}_{7-\delta}$,¹⁴ neutron scattering experiments on $\text{YBa}_2\text{Cu}_3\text{O}_{6.45}$,¹⁶ and especially scanning probe measurements on several materials.^{17,18}

We begin with definitions, which are important in this area because research on nematicity in strongly correlated systems is quickly developing field and perhaps as a

result the term has become broadly applied in some cases to phenomena that are rather common and do not fit under the standard definitions. The formal definition of a nematic phase is found in the theory of liquid crystals.¹⁹ There a mesomorphic (lacking long range order) liquid crystal is called *nematic* if the constituent anisotropic molecules have one preferential orientation axis. At the same time, the centers of molecules are disordered. In this sense, a nematic solid state phase would be a glass or a disordered alloy where short-range correlations in one direction are different from the other. This is illustrated in Fig. 1. The left panel shows an ordered orthorhombic crystal; note that the lattice parameters $a = b$, but the crystal symmetry is orthorhombic and a long range order is present. Such a state is not a nematic. Note also that the two species need not be different ions, they can just as well be spins on different sites. The middle panel shows a textured crystal where there is a long range order in one direction, but not in the other. Strictly speaking, this is not a nematic phase either. On the other hand, the right panel is an example of a canonical nematic phase: there is no long range order at all, yet the number of the like bonds along a is 70% larger than the number of the unlike bonds, while along b there is no such correlation. Such a crystal may show substantial anisotropy in *e.g.* transport properties. In fact, this is the signature of nematicity – a breaking of rotational symmetry without translational symmetry breaking.

Nematicity in the electronic subsystem may or may not trigger a significant difference between a and b depending on the relative energy scales associated with the nematic order and the lattice (i.e. elastic constants). For instance, a considerable anisotropy in transport is observed in the high field nematic phase of $\text{Sr}_3\text{Ru}_2\text{O}_7$ without any detectable a/b differentiation.²⁰ On the other hand, there is a strong structural signature at the onset of the very likely nematic phase that precedes the spin density wave transition as LaFeAsO is cooled.^{21,22} However, note that the spin density wave phase itself has long range translational symmetry breaking, and while it lowers the rotational (point group) symmetry from tetragonal to orthorhombic, it is not a nematic.

To summarize, the concept of electronic nematicity can

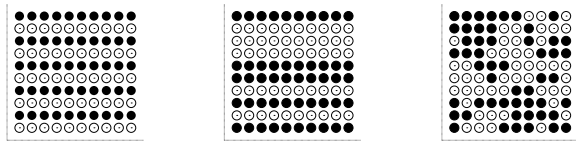


FIG. 1: Schematic depiction of different types of ordering in crystalline media: (a) Symmetry-breaking long range order; (b) Symmetry-breaking texture (long range order in one direction only); (c) nematic order. In the last case, there is no long-range ordering in any direction but the number of the like bonds along x is different from the number of unlike bonds, while along y there are the same number of like and unlike bonds.

and should be applied to crystalline solids to describe a situation where electronic or magnetic interactions cause the rotational symmetry to be spontaneously broken without long range positional or magnetic order. In fact, only one truly tetragonal cuprate, $(\text{Ca}, \text{Na})_2\text{CuO}_2\text{Cl}_2$, has been studied in this context, but only by scanning tunneling microscope (STM) based spectroscopy, which is a surface sensitive technique, and there is evidence that the surface may have a lower symmetry due to a reconstruction (see below). Therefore the issue is the more subtle one of whether there is an electronic instability of the CuO_2 planes towards a breaking of their four fold symmetry that drives the pseudogap. This must be distinguished from the possibility that specific probes are particularly sensitive to the pre-existing lack of four-fold symmetry of the lattice. This is complicated by the fact that electronic states around a gap or pseudogap are generally much more sensitive to anisotropy than the more dispersive bands that would be present prior to the gap-ping.

II. MATERIALS

When discussing electronic instabilities in complex materials, such as cuprates, it is important to keep in mind that electrons are charged particles. Therefore they are subject to the Coulomb interaction both with other electrons and with the ions that make up the crystal lattice. The effective strength of the interaction between quasi-particles at the crystal lattice is affected by screening. In fact, it is generally the case that different electronic states and different energies have different couplings to the lattice, as seen for example in mode and momentum dependent electron-phonon couplings. There is no a priori reason for assuming that such couplings are negligible, especially on low energy scales such as those associated with the pseudogap.

The shadow Fermi surfaces seen²³ in angle resolved photoemission spectroscopy (ARPES) measurements provide an instructive example. A low intensity replica of the Fermi surface of superconducting $\text{Bi}_2\text{Sr}_2\text{CaCu}_2\text{O}_{8+\delta}$ was observed shifted from the main

Fermi surface by $(\pi/a, \pi/a)$, which is the antiferromagnetic ordering vector of the undoped cuprates. This shadow was ascribed to scattering by antiferromagnetic fluctuations, which would be a novel electronic effect presumably related to strong correlations. This led to a large body of follow on experimental and theoretical work aimed at elucidating the detailed underlying mechanism. However, it was pointed out early on that the shadow bands were remarkably sharp for a fluctuation induced feature and that the lattices of the Bicuprates have structural distortions that include the cell doubling needed to produce this shadow.^{24,25} More recent experiments showed that this prosaic picture explains the shadow Fermi surface.^{26–28} Importantly, this distortion lowers the symmetry from tetragonal to orthorhombic and as evidenced by the observation of the shadow Fermi surface couples significantly to the electronic states involved in superconductivity and the pseudogap. Another instructive example is provided by the high sensitivity of superconductivity in the $(\text{La}, \text{Ba}, \text{Sr})_2\text{CuO}_4$ system to the structural phase transitions in particular the switching between low temperature orthorhombic (LTO) to the low temperature tetragonal (LTT) distorted structures with composition.²⁹

$\text{YBa}_2\text{Cu}_3\text{O}_{7-\delta}$ has two Cu-O systems, CuO_2 planes and $\text{CuO}_{1-\delta}$ linear chains. The apical O atoms of the plane Cu are also nearest neighbors of the chain Cu in this structure. This leads to hybridization between the bands at the Fermi surface that are derived from the plane Cu and electronic states associated with the chains, including near $\delta=0$, the chain Fermi surface.³⁰ The fact that there is coupling between these two electronic subsystems is seen from the relatively low anisotropy of the resistivity, ρ_c/ρ_{ab} , i.e. the relatively high c -axis conductivity as compared to other layered cuprates and also the opening of a substantial presumably induced superconducting gap on the chain derived Fermi surface. As mentioned, the $\text{CuO}_{1-\delta}$ layer consists of Cu-O-Cu chains. The chain formation is associated with O structural ordering, which takes place at high T and leads to an increasing orthorhombicity as the O increasingly order with decreasing T and annealing.^{31,32} This chain formation persists to low doping (high δ) and in fact at $\delta=0.5$ an ordered orthorhombic structure with alternating fully oxygenated chains and empty “chains” forms. High resolution x-ray scattering studies have shown that there is an interplay between this orthorhombicity and superconductivity, as reflected in an anomaly in b/a at T_c .³³ Importantly, substantial orthorhombicity persists with increasing δ up to the superconductor–antiferromagnet phase boundary.³²

$(\text{Ca}, \text{Na})_2\text{CuO}_2\text{Cl}_2$ is a true tetragonal material as was shown by neutron diffraction measurements.³⁴ However, the only experimental study pointing at nematicity in this material is by STM, which is surface sensitive. A low energy electron diffraction (LEED) image of the surface of this material was reported by Kohsaka and co-workers.³⁵ They do not find evidence for a reconstruction in their pattern. However, based on the intensity

of the Bragg peaks in the LEED pattern, it was not of sufficient quality to detect a surface reconstruction consisting of displacements of the surface atoms (see Refs. 36 and 37 for reviews of the LEED technique). Moreover, a strong shadow band is seen in ARPES, and as in the Bi compound discussed above, it is sharp in momentum space. This sharpness shows that it comes from a static order rather than fluctuations, which would introduce a width related to the momentum distribution of the fluctuations that provide the scattering. This shadow is then a strong indication that the surface is reconstructed. In fact, the ionic charges of Cl, Ca and Na are almost certainly -1, +2 and +1, respectively. There is then no natural neutral (001) cleavage plane in this crystal and so a reconstruction is highly likely. More careful investigation of this surface is suggested to determine the actual reconstruction pattern and its symmetry.

Finally, it is important to note that (1) an orthorhombic point group does not contain a four-fold axis and therefore regardless of sample orientation, measurement direction or coordinate system one cannot have a breaking of four-fold symmetry, since there is no four-fold axis to start with; and (2) the symmetry of a surface can be lower than the symmetry of the bulk, but it cannot be higher; in particular a (001) face of an orthorhombic crystal will not have four-fold symmetry.

III. SCANNING TUNNELING MICROSCOPY BASED SPECTROSCOPY

We start with STM, as these experiments have been most emphasized in connection with possible nematicity. The systems studied include Bi-2212 phases and $(\text{Ca,Na})_2\text{CuO}_2\text{Cl}_2$.^{17,18,38} Importantly, $(\text{Ca,Na})_2\text{CuO}_2\text{Cl}_2$ is the only cuprate that has been studied in the context of nematicity at T^* and is at the same time crystallographically tetragonal in bulk. The measurements are done at low T , well below T^* . Spectra are taken as a function of tip position and two energy scales are identified in the spectra: Δ_0 , which is related to superconductivity and Δ_1 , which is associated with the pseudogap. $\Delta_1(\mathbf{r})$ is found to vary considerably with position \mathbf{r} on the sample surface. This indicates a sensitivity of electronic states Δ_1 at the pseudogap edges to the local chemistry or structure variations on the surface. This is as expected because states at and near a gap edge are in general heavier than those associated with dispersive states, and therefore more easily localized. This helps to confirm the association of Δ_1 with the pseudogap. Real space images of the spectra with the intensity of $Z(\mathbf{r}, E)$, which is the ratio of differential conductances and opposite bias, defined in Ref. 18, also show variations, and these are correlated with the variations in Δ_1 , so that real space plots of $f(\mathbf{r}) = Z(\mathbf{r}, \Delta_1(\mathbf{r}))$ show strong spatial dependence. What is being plotted then is a function that has the most inhomogeneity in real space presumably because of it has the most sensitivity

to variations in local structure and chemistry.

As emphasized in the STM papers, this function shows chain-like correlations running along the directions of the Cu-O-Cu bonds with lengths of several atoms. As mentioned the structures of Bi-cuprates have strong lattice distortions. They consist of shifts of O atoms in the Bi-O planes by ~ 0.5 Å, as well as large mainly transverse shifts of the apical O and buckling of the CuO_2 planes, corresponding to tilts of the CuO_6 octahedra. Such tilt type instabilities come from shifts of the O atoms and not the cations. There is also an incommensurate modulation associated with the mismatch between the Bi-O and CuO_2 systems.³⁹ Further, the $\text{Bi}^{3+}\text{-O}^{2-}$ surface is not charge neutral and therefore additional distortions may be expected, although these have not been quantified experimentally. In any case, tilt instabilities in perovskites are well studied.⁴⁰ Layered perovskite zone corner lattice instabilities with tilts around [110] are close in energy to structures with [100] tilts. Also, because of the bonding topology, in particular the square network of corner sharing octahedra the tilts of nearby octahedra are generally correlated. In other words, clockwise rotation of an octahedra drives counterclockwise rotation of its neighbors because of the shared O atoms. This is seen in the phonon dispersions of perovskites, where for example in cubic perovskites the R_{25} branch disperses weakly towards the M point but strongly towards Γ (see e.g. Ref. 41 for a discussion of this).

These tilts, which are strong in Bi-cuprates, provide a natural explanation for chain-like correlations seen in the STM experiments if (1) local disorder on the surface is strong enough to rotate the tilt axes away from [110] towards [100] or [010] and (2) this couples to the electronic structure being measured. In regard to (1), we note that the STM images for the underdoped sample show substantial disorder, besides the chain-like correlations. Visually, this appears stronger in the spectroscopic maps that show the electronic structure of the Cu-O system, and is therefore sensitive to O position than in the topographic image (Fig. 4d of Ref. 18, which shows the Bi positions). To quantify this, we took the STM images of the spectroscopy Z functions showing the chains (Figs. 4a, 4b and 4e) of Kohsaka and co-workers,¹⁸ and Fourier transformed (FT) it. The resulting transforms is shown in Fig. 2. Only the first three Bragg reflections (100), (110), and (200) are clearly seen and these are broad and fall off rapidly with order. Note that even with strong variations in the intensities of the STM image from site to site, if the atoms were on periodic sites Bragg peaks should be seen up to higher order although they may be broadened, similar to what is seen in x-ray crystallography for alloys. The FT instead indicates shifts of the atoms from the periodically arranged sites in the bulk. In regard to (2) we note that the Fermi surface comes from Cu $d_{x^2-y^2}$ - O p_σ anti-bonding states, and the O p orbitals (x, y, z) are orthogonal. This is manifested in the shape of the Fermi surface which is flat near the nodal directions. A square Fermi surface can be regarded as the

intersection of segments of two one dimensional Fermi surfaces, and so if one concentrates on the nodal regions that provide the gap edge states around Δ_1 , one has the intersection of two one dimensional surfaces, one along x and the other along y . The σ hopping matrix elements are reduced quadratically as the bond angle deviates from 180° , providing a mechanism for coupling of the gap edge states to the tilts. As noted, the states at the Fermi surface are known to couple to the tilts as evidenced by the shadow Fermi surface, and focusing on the states at the edge of the pseudogap is expected to enhance this sensitivity as discussed. Therefore, the images shown in the STM experiments can have a rather prosaic explanation.

Returning to chain-like correlations in perovskites, we mention that an analogous situation can occur in the lattice dynamics of the soft mode of ferroelectric perovskites such as BaTiO_3 and KNbO_3 .^{42,43} The real space interactions for the soft mode have a one-dimensional character, leading to chain-like correlations seen in diffuse scattering experiments above the Curie temperature. These correlations are of comparable length to the chains in the STM images, although unlike them they are dynamic rather than static. These are cubic crystals, not nematics, since the correlated chains run equally along all three Cartesian directions. Similarly, even though each molecule in a liquid of rod-like molecules may have a certain orientation that correlates with its neighbors it is not a liquid crystal unless the global rotational symmetry is lost.

Examining the FT image (Fig. 2), one notes that there is no clear breaking of $x - y$ symmetry. This means that the surface is not obviously nematic on the scale of the STM image shown (~ 30 Cu spacings on a side). One may ask if the image is a superposition of small nematic domains. In fact, one can find regions in the image where two or more neighboring chains appear to run together along the same direction. However, one can also find regions with a single chain. The FT image shows diffuse intensity along the $H0$ and $0K$ directions reflective of chain-like correlations (see Ref. 42, but it is not clear that other streaks expected are present, nor is there an strong asymmetry above the noise level in the shape of e.g. the 10 Bragg peak that would indicate local nematic domains. We conclude that at least in this image such regions, if present above a statistical level, are very small.

IV. TRANSPORT

The Nernst coefficient, ν , is a very sensitive probe of gapping.^{44,45} Like the thermopower, it is proportional to T at low T and in a simple band structure it is inversely proportional to the distance of the band edge from the Fermi energy. Unlike the thermopower, ν is proportional to the mobility, and electron and hole contributions are additive. Large Nernst effects are found in semimetals, with Bi being a good example,⁴⁴ while, in normal metals the Nernst coefficient is very small. Therefore, in a pseudogapped system one expects the Nernst coefficient

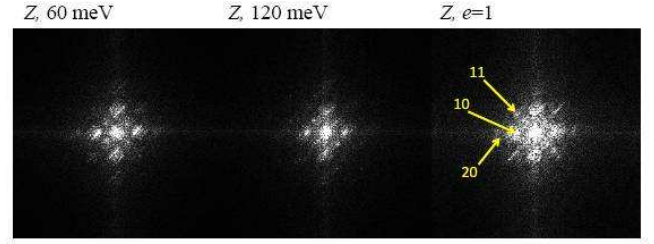


FIG. 2: (color online) FFT of Figs. 4a (left), 4b (middle) and 4e (right), from Ref. 18, with low order Bragg positions indicated. The FFT was done on the figure converted to greyscale after trimming a border at the top to remove the caption and slivers from the left and right to compensate the top border thus yielding square images.

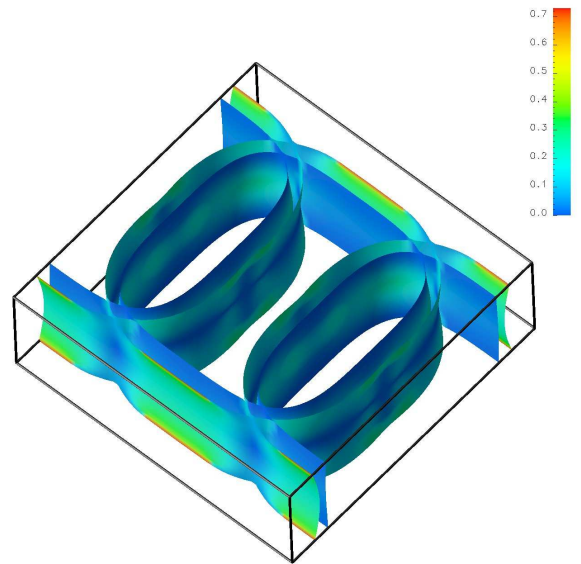


FIG. 3: (color online) Calculated Fermi surface of $\text{YBa}_2\text{Cu}_3\text{O}_{6.5}$ showing the plane derived sections only (see text). There are two barrel shaped sections corresponding to the two CuO_2 planes in the structure and additionally a zone folding due to the alternation of filled and empty chains in the $\text{CuO}_{1-\delta}$, $\delta = 0.5$ layer.

cient to grow strongly as regions of the Fermi surface in the nodal directions are increasingly removed from participation in transport, consistent with what was found experimentally.¹⁴ On the level of the standard Boltzmann kinetic theory with a single relaxation rate, the Nernst coefficient is defined by derivatives of the transport function with respect to the chemical potential, similarly to the Seebeck coefficient.^{44,46} Thus, the Nernst coefficient is particularly sensitive to those parts of the Fermi surface that most rapidly change with the energy. We show the plane derived sections of the Fermi surface of $\text{YBa}_2\text{Cu}_3\text{O}_{6.5}$ in Fig. 3. These were obtained with

the general potential linearized augmented plane wave method⁴⁷ as implemented in the WIEN2k code,⁴⁸ using the generalized gradient approximation of Perdew, Burke and Ernzerhof.⁴⁹ Our Fermi surface is similar to that reported previously by Carrington and Yelland.⁵⁰ For the present discussion, we have removed the chain derived Fermi surface from plot and colored the remaining Fermi surfaces according to the local transport function, that is, the squared Fermi velocity. We see that despite the fact that the Fermi surface geometry retains the approximate tetragonal symmetry, the transport function appears quite anisotropic, with some area of heavy electrons at the “y” faces, but not “x” faces. From this plot it is clear that hybridization with chain Cu-O system can make transport properties, especially the Nernst coefficient, quite anisotropic, even if one excludes the transport in the CuO chains themselves.

Indeed, Ando and co-workers⁵¹ have measured the resistivity of de-twinned $\text{YBa}_2\text{Cu}_3\text{O}_{7-\delta}$ crystals as a function of oxygen content and temperature. They find that the resistivity is anisotropic in all samples, including $\delta=0$, and that in underdoped samples ($\delta=0.55$ and $\delta=0.35$) the resistivity anisotropy increases with decreasing temperature. The resistivity for high doping ($\delta=0$ and $\delta=0.17$) is qualitatively different from the underdoped samples, presumably reflecting the fact that the $\text{CuO}_{1-\delta}$ chains no longer contribute significantly to the conductivity so that, as discussed by Ando and co-workers, the anisotropy reflects anisotropy of the CuO_2 planes. Importantly, the anisotropy is a smooth function of temperature up to the highest reported $T=300\text{K}$, which is well above T^* , and furthermore shows no clearly apparent structure that can be associated with the pseudogap, although the pseudogap T^* can be mapped from analysis of the T dependent curvature of the resistivity.⁵² This is consistent with the view that the observed anisotropy is a one-electron effect reflecting the anisotropy of the in-plane Fermi velocity induced by the hybridization with chains.

On the other hand, the scattering rate may also be anisotropic (even if the chain electrons are localized, they can still affect the scattering rates). In fact, optical conductivity measurements suggest an anisotropy in the scattering rate that behaves similarly above and below T^* .⁵³ Either way, it is clear that the observed anisotropy in ν likely arises from anisotropy in the electronic structure that exists independent of T^* , which manifests itself particularly strongly in ν , at low T , where the gapping is strong. Therefore, while the Nernst anisotropy, may, of course, indicate a symmetry breaking, a simpler explanation in terms of the always present anisotropy of the underlying electronic structure, enhanced at low temperature by gapping is not at all excluded.

V. NEUTRON SCATTERING

Inelastic neutron scattering offers a number of advantages. It is a true bulk sensitive probe and it directly

measures the dissipative part of the magnetic susceptibility, χ'' as a function of momentum and energy. Hinkov and co-workers¹⁶ reported such measurements for de-twinned crystals of underdoped $\text{YBa}_2\text{Cu}_3\text{O}_{6.45}$. They showed by analysis of the H,K,L dependent structure factors that the magnetic response that they measure is from the CuO_2 planes and not the chain Cu. As expected they find inelastic scattering near the $(1/2,1/2)$ position corresponding to the antiferromagnetic ordering vector of the undoped compounds. At high energy (50 meV) the distribution of χ'' around this momentum is isotropic but as the energy is lowered below 7 meV they find an anisotropy that increases as the energy is lowered towards the quasielastic regime (3 meV). The scattering is elongated along the a^* direction, indicating the presence of chain-like magnetic correlations along the b direction. This anisotropy was found to be strongly T dependent and vanishes below 100 K. This very interesting behavior, i.e. the development of 1D magnetic correlations in the CuO_2 planes as T is lowered could be an indication of nematicity, or it could be interpreted as nearness to magnetism in an anisotropic (orthorhombic) material. Clearly, further investigation is needed. However, one issue that should be emphasized is that the anisotropy is already absent when the temperature is raised to 100 K, while T^* for this composition is at much higher $T \sim 250\text{K}$.⁵² This calls into question the relationship between this anisotropy and the pseudogap. One experiment that would be particularly interesting would be inelastic neutron measurements for a truly tetragonal material such as $(\text{Ca},\text{Na})_2\text{CuO}_2\text{Cl}_2$ when suitable samples become available.

VI. SUMMARY

In summary, we argue based on symmetry and other considerations that the existing experimental data are not sufficient to prove a nematic origin of the pseudogap in cuprates. Bulk sensitive measurements on tetragonal materials, while difficult, will be very helpful in establishing whether the phase below T^* is associated with the onset of nematic order.

Acknowledgments

This work was supported by the Department of Energy, Materials Sciences and Engineering Division (DJS) and the Office of Naval Research (IIM).

- ¹ W. W. Warren, Jr., R. E. Walstedt, G. F. Brennert, R. J. Cava, R. Tycko, R. F. Bell, and G. Dabbagh, Phys. Rev. Lett. **62**, 1193 (1989).
- ² H. Alloul, T. Ohno, and P. Mendels, Phys. Rev. Lett. **63**, 1700 (1989).
- ³ H. Ding, T. Yokoya, J. C. Campuzano, T. Takahashi, M. Randeria, M. R. Norman, T. Mochiku, K. Kadowaki, and J. Giapintzakis, Nature (London) **382**, 6586 (1996).
- ⁴ J. L. Tallon and J. W. Loram, Physica C **349**, 53 (2001).
- ⁵ M. R. Norman, D. Pines, and C. Kallin, Adv. Phys. **54**, 715 (2005).
- ⁶ V. Aji and C. M. Varma, Phys. Rev. B **75**, 224511 (2007).
- ⁷ Y. Li, V. Baledent, N. Barisic, Y. Cho, B. Fauque, Y. Sidis, G. Yu, X. Zhao, P. Bourges, and M. Greven, Nature (London) **455**, 372 (2008).
- ⁸ A. Kanigel, U. Chatterjee, M. Randeria, M. R. Norman, G. Koren, K. Kadowaki, and J. C. Campuzano, Phys. Rev. Lett. **101**, 137002 (2008).
- ⁹ T. Yoshida, M. Hashimoto, S. Ideta, A. Fujimori, N. Manella, Z. Hussain, Z. Y. Shen, M. Kubota, K. Ono, S. Komiya, et al., Phys. Rev. Lett. **103**, 037004 (2009).
- ¹⁰ T. Kondo, R. Khasanov, T. Takeuchi, J. Schmalian, and A. Kaminski, Nature (London) **457**, 296 (2009).
- ¹¹ E. Fradkin and S. A. Kivelson, Science **327**, 155 (2010).
- ¹² S. A. Kivelson, E. Fradkin, and V. J. Emery, Nature (London) **393**, 550 (1998).
- ¹³ M. Vojta, Adv. Phys. **58**, 699 (2009).
- ¹⁴ R. Daou, J. Chang, D. LeBoeuf, O. Cyr-Choiniere, F. Laliberte, N. Dorion-Leyraud, B. J. Ramshaw, R. Liang, D. A. Bonn, W. N. Hardy, et al., Nature (London) **463**, 519 (2010).
- ¹⁵ A. Hackl and M. Vojta, Phys. Rev. B **80**, 220514(R) (2009).
- ¹⁶ V. Hinkov, D. Haug, B. Fauque, P. Bourges, Y. Sidis, A. Ivanov, C. Bernhard, C. T. Lin, and B. Keimer, Science **319**, 597 (2008).
- ¹⁷ Y. Kohsaka, C. Taylor, K. Fujita, A. Schmidt, C. Lupien, T. Hanaguri, M. Azuma, M. Takano, H. Eisaki, H. Takagi, et al., Science **315**, 1380 (2007).
- ¹⁸ Y. Kohsaka, C. Taylor, P. Wahl, A. Schmidt, J. Lee, K. Fujita, J. W. Alldredge, K. McElroy, J. Lee, H. Eisaki, et al., Nature (London) **454**, 1072 (2008).
- ¹⁹ P. G. de Gennes and J. Prost, *The Physics of Liquid Crystals, 2nd Edition* (Oxford Science Publications, 1993).
- ²⁰ R. A. Borzi, S. A. Grigera, J. Farrell, R. S. Perry, S. J. S. Lister, S. L. Lee, D. A. Tennant, Y. Maeno, and A. P. Mackenzie, Science **315**, 214 (2007).
- ²¹ C. de la Cruz, Q. Huang, J. W. Lynn, J. Y. Li, W. Ratcliff II, J. L. Zarestsky, H. A. Mook, G. F. Chen, J. L. Luo, N. L. Wang, et al., Nature (London) **453**, 899 (2008).
- ²² I. I. Mazin and M. D. Johannes, Nature Physics **5**, 141 (2009).
- ²³ P. Aebi, J. Osterwalder, P. Schwaller, L. Schlapbach, M. Shimoda, T. Mochiku, and K. Kadowaki, Phys. Rev. Lett. **72**, 2757 (1994).
- ²⁴ D. J. Singh and W. E. Pickett, Phys. Rev. B **51**, 3128 (1995).
- ²⁵ D. J. Singh and W. E. Pickett, J. Supercond. **8**, 583 (1995).
- ²⁶ A. Koitzsch, S. V. Borisenko, A. A. Kordyuk, T. M. Kim, M. Knapfer, J. Fink, M. S. Golden, W. Koops, H. Berger, B. Keimer, et al., Phys. Rev. B **69**, 220505(R) (2004).
- ²⁷ K. Nakayama, T. Sato, T. Dobashi, K. Terashima, S. Souma, H. Matsui, T. Takahashi, J. C. Campuzano, K. Kudo, T. Sasaki, et al., Phys. Rev. B **74**, 054505 (2006).
- ²⁸ A. Mans, I. Santoso, Y. Huang, W. K. Siu, S. Tavadod, V. Arpiainen, M. Lindroos, H. Berger, V. N. Strocov, M. Shi, et al., Phys. Rev. Lett. **96**, 107007 (2006).
- ²⁹ M. K. Crawford, W. E. Farneth, E. M. McCarron, III, R. L. Harlow, and A. H. Moudden, Science **250**, 1390 (1990).
- ³⁰ W. E. Pickett, H. Krakauer, R. E. Cohen, and D. J. Singh, Science **255**, 46 (1992).
- ³¹ B. W. Veal, A. P. Paulikas, H. You, H. Shi, Y. Fang, and J. W. Downey, Phys. Rev. B **42**, 6305 (1990).
- ³² R. Liang, D. A. Bonn, W. N. Hardy, J. C. Wynn, K. A. Moler, L. Lu, S. Laroche, L. Zhou, M. Greven, L. Lurio, et al., Physica C **383**, 1 (2002).
- ³³ P. M. Horn, D. T. Keane, G. A. Held, J. L. Jordan-Sweet, D. L. Kaiser, F. Holtzberg, and T. M. Rice, Phys. Rev. Lett. **59**, 2772 (1987).
- ³⁴ D. N. Argyriou, J. D. Jorgensen, R. L. Hitterman, Z. Hiroi, N. Kobayashi, and M. Takano, Phys. Rev. B **51**, 8434 (1995).
- ³⁵ Y. Kohsaka, T. Sasagawa, F. Ronning, T. Yoshida, C. Kim, T. Hanaguri, M. Azuma, M. Takano, Z. X. Shen, and H. Takagi, J. Phys. Soc. Japan **72**, 1018 (2003).
- ³⁶ M. A. Van Hove, W. Moritz, H. Over, P. J. Rous, A. Wander, A. Berbieri, N. Materer, U. Starke, and G. A. Somorjai, Surf. Sci. Rep. **19**, 191 (1993).
- ³⁷ K. Heinz, Rep. Prog. Phys. **58**, 637 (1995).
- ³⁸ T. Valla, A. V. Fedorov, J. Lee, J. C. Davis, and G. D. Gu, Science **314**, 1914 (2006).
- ³⁹ Y. Le Page, W. R. McKinnon, J. M. Tarascon, and P. Barboux, Phys. Rev. B **40**, 6810 (1989).
- ⁴⁰ A. M. Glazer, Acta Crystallogr. Sect. B **28**, 3384 (1972).
- ⁴¹ M. Ghita, M. Fornari, D. J. Singh, and S. V. Halilov, Phys. Rev. B **72**, 054114 (2005).
- ⁴² R. Comes, M. Lambert, and A. Guinier, Solid State Commun. **6**, 715 (1968).
- ⁴³ R. Yu and H. Krakauer, Phys. Rev. Lett. **74**, 4067 (1995).
- ⁴⁴ K. Behnia, M. A. Measson, and Y. Kopelevich, Phys. Rev. Lett. **98**, 076603 (2007).
- ⁴⁵ J. Chang, R. Daou, C. Proust, D. LeBoeuf, N. Dorion-Levaurd, F. Laliberte, B. Pingault, B. J. Ramshaw, R. Liang, D. A. Bonn, et al., Phys. Rev. Lett. **104**, 057005 (2010).
- ⁴⁶ J. M. Ziman, *Electrons and Phonons* (Clarendon, Oxford, 1960).
- ⁴⁷ D. J. Singh and L. Nordstrom, *Planewaves, Pseudopotentials and the LAPW Method, 2nd Ed.* (Springer Verlag, Berlin, 2006).
- ⁴⁸ P. Blaha, K. Schwarz, G. Madsen, D. Kvasnicka, and J. Luitz, WIEN2k, An Augmented Plane Wave + Local Orbitals Program for Calculating Crystal Properties (K. Schwarz, Tech. Univ. Wien, Austria) (2001).
- ⁴⁹ J. P. Perdew, K. Burke, and M. Ernzerhof, Phys. Rev. Lett. **77**, 3865 (1996).
- ⁵⁰ A. Carrington and E. A. Yelland, Phys. Rev. B **76**, 140508(R) (2007).
- ⁵¹ Y. Ando, K. Segawa, S. Komiya, and A. N. Lavrov, Phys. Rev. Lett. **88**, 137005 (2002).
- ⁵² Y. Ando, S. Komiya, K. Segawa, S. Ono, and Y. Kurita, Phys. Rev. Lett. **93**, 267001 (2004).

- ⁵³ Y. S. Lee, K. Segawa, Y. Ando, and D. N. Basov, Phys. Rev. B **70**, 014518 (2004).